

Low-temperature ultrasonic study of trapped hydrogen in niobium

D. B. Poker, G. G. Setser, and A. V. Granato

*Department of Physics and Materials Research Laboratory, University of Illinois at Urbana-Champaign,
Urbana, Illinois 61801*

H. K. Birnbaum

*Department of Metallurgy and Materials Research Laboratory, University of Illinois at Urbana-Champaign,
Urbana, Illinois 61801*

(Received 15 August 1983)

The elastic constants and attenuation of niobium containing low concentrations of oxygen and hydrogen (deuterium) have been measured between 0.5 and 15 K, as a function of temperature, frequency, polarization, and hydrogen isotope. Two relaxations were observed for the C' mode. No observable relaxations appeared in C_{44} or the bulk modulus. At 10 MHz the relaxations occurred at 2.5 and 5.5 K for H, shifting to higher temperature for D. The relaxation strength of the low-temperature process is linear in H concentration, while the higher-temperature process is nonlinear. The low-temperature process exhibits an apparent activation energy of 1.8 meV, with a nonclassical temperature dependence of the relaxation strength. The constraints which these results place upon a delocalized-wave model are discussed.

INTRODUCTION

Evidence for tunneling of H in Nb was obtained by Sellers, Anderson, and Birnbaum¹ from measurements of specific heat showing a large isotope effect below 1 K. It was found by Morkel, Wipf, and Neumaier² that the specific-heat anomaly was caused by hydrogen trapped at interstitial impurities. Many other measurement techniques have also been applied to this system (internal friction,³⁻¹² x-ray scattering,¹³ neutron scattering, channeling, muon-spin relaxation,¹⁴⁻²¹ thermal,²²⁻²³ and electrical resistance²⁴), but as yet no generally accepted model for the defect configuration has resulted.

We report here²⁵ measurements of ultrasonic attenuation and velocity at low temperatures in dilute Nb-O-H single-crystal alloys as a function of temperature, frequency, polarization, and isotope and impurity concentration. A relaxation peak near 2.5 K at 10 MHz is found with an unusual isotope dependence. The properties of this peak provide important clues and restrictions for any model for the configuration, particularly concerning the symmetry and number of eigenstates required.

EXPERIMENTAL TECHNIQUE

Cubic samples slightly larger than 1 cm were spark-cut with one set of (100) faces and two sets of (110) faces. The faces were mechanically polished using diamond paste abrasive and were measured to be flat to within one wavelength of sodium light with opposite faces parallel to within 3×10^{-5} rad. Mass-spectrographic analysis indicated the following impurity concentration in at. ppm before the final anneal: Ta, 200; C, 70; O, 64; N, 40; Cl, 9; all others, less than 3.

One sample was annealed at 1800 C in an atmosphere of 0.1 mPa oxygen to remove carbon and nitrogen impuri-

ties. The pressure was increased to 0.26 mPa for a period of 5 h to introduce approximately 1000 ppm of oxygen. Hydrogen and deuterium were introduced by gas-charging at about 800 C. Measurement of H concentrations by vacuum-outgassing after completion of the experiments provided a check of the concentration.

Ultrasonic pulses were generated and detected with 10-MHz quartz transducers cut for shear and longitudinal modes of propagation. The transducers were bonded to the sample using Nonaq stopcock grease. Measurements were made of the elastic constants C_{11} , C_{44} , and C' by varying the orientation and polarization of the transducers.

Attenuation was measured using a Matec model-6000 pulse-echo generator and model-2470A attenuation recorder. Velocity was measured using a pulsed-echo superposition system²⁶ having a sensitivity of one part in 10^7 . The relative change in velocity $\Delta v/v$ is proportional to the frequency change $\Delta f/f$ which is related to the elastic-constant change $\Delta C/C = 2\Delta f/f$.

ANELASTIC RELAXATION

The introduction of a defect into a lattice produces a distortion in the positions of the neighboring atoms with the distortion reflecting the symmetry of the site in the lattice. The distortion can be represented by a strain tensor

$$\lambda_{ij}^{(p)} = \frac{\partial \epsilon_{ij}}{\partial C_p}, \quad (1)$$

where ϵ_{ij} are the components of strain introduced by the defect and C_p is the concentration of defects in the p th orientation. The change in decrement δ and elastic con-

stant $\delta C/C$ due to the defect is given by the Debye equations

$$\delta = \pi\omega\tau\Delta/(1+\omega^2\tau^2), \quad \delta C_{ij}/C_{ij} = \Delta/(1+\omega^2\tau^2) \quad (2)$$

where ω is the frequency of the applied stress, τ is the relaxation time for the defect, and the relaxation strength Δ is given by

$$\Delta = \beta\Omega C_0 C_{ij}(\delta\lambda)^2/k_B T, \quad (3)$$

where β is a dimensionless geometric constant of order unity, C_0 is the total concentration of defects, Ω is the atomic volume, k_B is Boltzmann's constant, and T is the temperature. C_{ij} is the corresponding elastic constant, and $\delta\lambda$ is the difference in the λ tensor between defect orientations.²⁷

EXPERIMENTAL RESULTS

Specimen Nb1 was charged with oxygen to a concentration of approximately 1000 ppm and experiments were conducted using various concentrations of hydrogen and deuterium. Nb2 was not charged with oxygen, but analysis showed a concentration of about 200 ppm of oxygen, carbon, and nitrogen combined. Relaxations were observed in the C' mode in samples charged with oxygen and hydrogen, but were not observed in the same samples charged only with oxygen. No relaxations were observed in the C_{44} mode under any conditions for specimens charged with either hydrogen or deuterium.

LOW-CONCENTRATION RESULTS

The C' mode velocity and decrement per unit concentration at 10 MHz for low concentrations of hydrogen and deuterium in Nb1 are shown in Fig. 1. Curve *A* represents the low-temperature velocity change of uncharged Nb, and is characteristic of most metals. The curve approaches the vertical axis with zero slope, while at higher temperatures it decreases with terms proportional to T^2 and T^4 .

The effect of adding 160 ppm of hydrogen upon the velocity is shown by curve *B*, while the effect of 200 ppm of hydrogen upon the decrement is shown by curve *C*. The velocity change due to hydrogen is negative and decreases as $1/T$ at high temperature. Between 3 and 2 K the velocity increases, while a peak in the decrement occurs, the normal behavior for a relaxation. However, below 2 K the velocity again starts to decrease with no corresponding effect in the decrement. The change in velocity is quite small, amounting to a change of 20 ppm at the lowest temperature.

The effect of adding 230 ppm of deuterium upon the velocity and decrement per unit concentration is shown by curves *D* and *E*, respectively. The relaxation is shifted to a higher temperature compared to hydrogen, but is much broader in temperature than the hydrogen relaxation. The velocity decreases below 2 K, as with hydrogen, but at higher temperatures the dispersion in the velocity continues through the superconducting transition around 9 K. The shift of the deuterium relaxation to higher tempera-

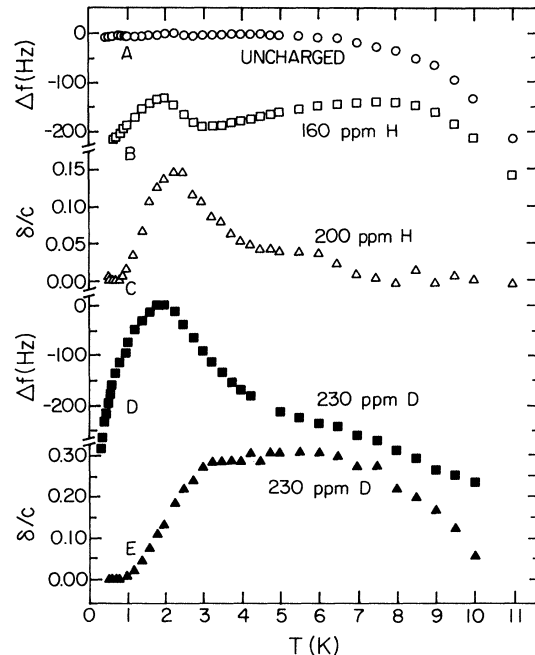


FIG. 1. Frequency change and decrement per unit concentration vs temperature for hydrogen and deuterium in niobium for a 10-MHz C' mode elastic wave.

tures compared to hydrogen suggests that the deuterium relaxes more slowly than hydrogen in this temperature range as with the isotope effects in diffusivity measured at higher temperatures.⁴ However, the width of the relaxation suggests that the deuterium relaxation frequency changes more slowly with temperature than does hydrogen, unlike the diffusivity results. The increased relaxation strength of deuterium allows more accurate measurements of C_{11} and C' , so that the bulk modulus can be calculated. If the bulk modulus change is zero, then

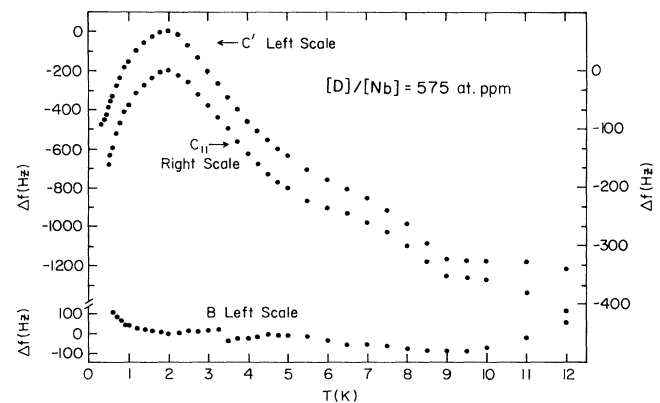


FIG. 2. C' , C_{11} , and B -mode frequency changes as functions of temperature for $[D]/[Nb]=575$ at. ppm. C' data are plotted against the upper left scale, while B data are plotted against the lower left scale. C_{11} data are plotted against the right scale. C' and C_{11} scales are in a ratio of 3:1 showing that parallel C' and C_{11} scales give no B relaxation. Origins of the C' and C_{11} scales are offset to permit easier viewing.

$$\delta B = 3\delta C_{11} - 4\delta C' = 0, \quad (4)$$

$$\delta C_{11}/C_{11} = 0.32\delta C'/C', \quad (5)$$

so the change in C_{11} should be about one-third the relative change in C' . The curves in Fig. 2 show C' and C_{11} with a factor-of-3 difference in scale, offset slightly to allow easier viewing. The bulk modulus is also shown, with no observable relaxation occurring above 1 K.

These results for low concentrations of hydrogen and deuterium indicate the presence of a relaxation occurring at 2.4 K at 10 MHz for hydrogen and at about 5 K at 10 MHz for deuterium. The deuterium relaxation has a larger strength for comparable concentrations and is much broader in temperature than for hydrogen. The relaxation strength for both isotopes is small, typically 0.1 ppm for 1 ppm of defects. This is 2–3 orders of magnitude smaller than is typical for point defects, but the sensitivity of the measurements is sufficient to measure the effects accurately.

HIGH-CONCENTRATION RESULTS

The concentration and polarization dependence of the hydrogen relaxation in Nb1 can be seen in Fig. 3. The curve representing the C' mode at a hydrogen concentration of 200 ppm is the same as curve C of Fig. 1. Increasing the concentration of hydrogen to 2150 ppm produces little change in the relaxation peak at 2.5 K per unit hydrogen concentration, indicating that the relaxation strength for the process is linearly dependent upon hydrogen concentration. However, a second relaxation, which can be seen as only a shoulder on the low-concentration curve becomes a separate peak on the high-concentration curve. With the use of the two concentrations for which

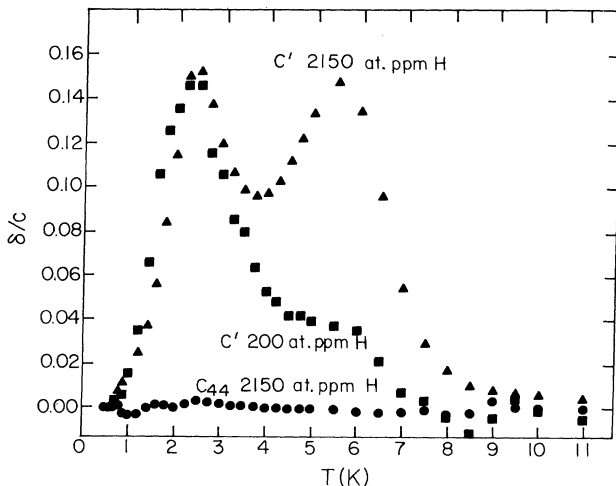


FIG. 3. Decrement of the C' mode per unit concentration as a function of temperature for $[H]/[Nb]=200$ and 2150 at. ppm. Low-temperature peaks match, indicating a linear temperature dependence. High-temperature peak has a concentration dependence which is nearly quadratic. Also shown is the decrement of the C_{44} mode per unit concentration for $[H]/[Nb]=2150$ at. ppm, indicating the relative absence of a relaxation in that mode.

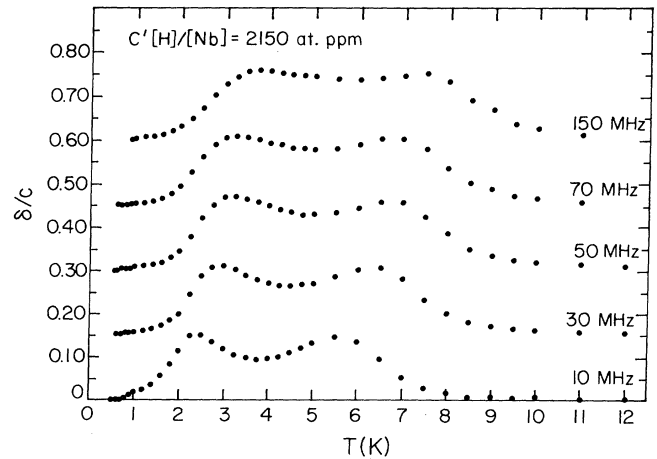


FIG. 4. Decrement of the C' mode per unit concentration as a function of temperature for $[H]/[Nb]=2150$ at. ppm at 10, 30, 50, 70, and 150 MHz. Horizontal axis of each successive curve has been displaced upward by 0.15 to permit easier viewing.

data is available, it is possible to calculate that the relaxation strength of the high-temperature relaxation depends upon hydrogen concentration to the 1.9 power, assuming a power-law dependence. This suggests that the relaxation, which appears near 6 K at 10 MHz is due to hydrogen pairs, which are either isolated or trapped at an interstitial oxygen solute.

The measurement of the decrement per unit concentration for the C_{44} mode is also indicated in Fig. 3 for comparison. No relaxation peak is evident, restricting the maximum C_{44} relaxation strength to 2 orders of magnitude below the C' value.

The effect on the C' relaxation of varying the ultrasonic frequency can be seen in Fig. 4. Both relaxation peaks shift to higher temperatures and become broader with increasing frequency.

Sample Nb1 was vacuum-annealed to remove any hydrogen, and then was charged with 1800 ppm of deuterium.

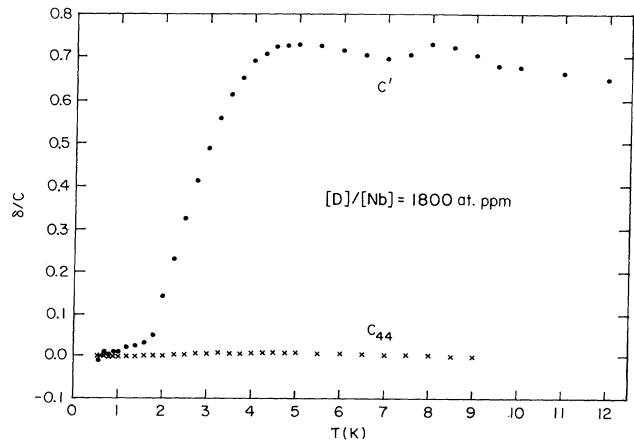


FIG. 5. Decrement of the C' and C_{44} modes per unit concentration as functions of temperature for $[D]/[Nb]=1800$ at. ppm. Two relaxations appear in the C' mode, while none occurs in the C_{44} mode.

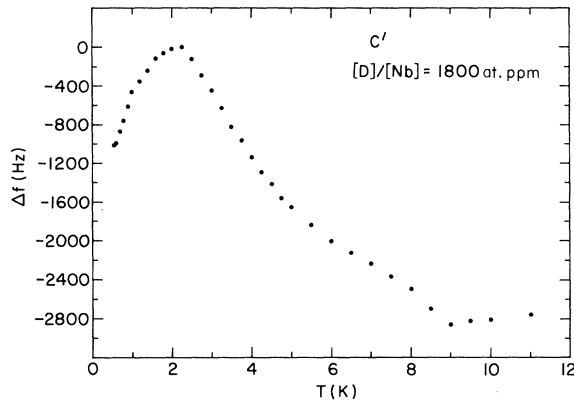


FIG. 6. Frequency change of the C' mode as a function of temperature for $[D]/[Nb]=1800$ at. ppm.

um. A comparison of both C' - and C_{44} -mode results is shown in Fig. 5. Here, as in the case of hydrogen, no relaxation is seen in C_{44} , but there is a relaxation in C' which has a larger relaxation strength than the C' relaxation with hydrogen. The decrement curve is extremely broad, as in the low-concentration case.

The velocity of the C' mode with the high concentration of deuterium is indicated in Fig. 6. In contrast to a high-concentration hydrogen velocity curve (not shown), where two distinct dispersions are obtained, there appear to be a single broad dispersion due to deuterium. Upon close examination it can be seen that one dispersion occurs between 2.5 and 5 K. Above 5 K the slopes of the velocity curve appear to be decreasing before increasing sharply again around 8 K. The discontinuity in slope between 9 and 9.5 K is due to the superconducting effect, and makes the behavior of the velocity curve above 9 K difficult to interpret. As in all other velocity measurements, there is a decrease in the velocity below 2 K with no corresponding decrement effect.

EFFECT OF COOLING RATE

In the process of data reduction, it was noticed that the relaxation strength of various modes would vary by as much as 50% between seemingly identical experiments. Since the relaxation strength is proportional to concentration by Eq. (3), a variation of the defect concentration from experiment to experiment would explain the anomaly. It has been suspected that the amount of hydrogen associated with oxygen would depend upon the cooling rate between 200 and about 70 K. To test this hypothesis, the following experiment was performed. The C' decrement in Nb1 containing 2150 ppm hydrogen was measured after cooling at the normal rate, about 1 K/min. The relaxation strength measured was typical of this type of experiment, as shown by the circles of Fig. 7. The sample was warmed to 150 K for 1 h to allow hydrogen to dissociate and precipitate as a hydride. It was then cooled rapidly, about 10 K/min to helium temperature. The decrement was then a factor of 2 lower, as shown by the squares of Fig. 7. The sample was then warmed to about 250 K, which was above the hydride solvus, for 1 h to allow the

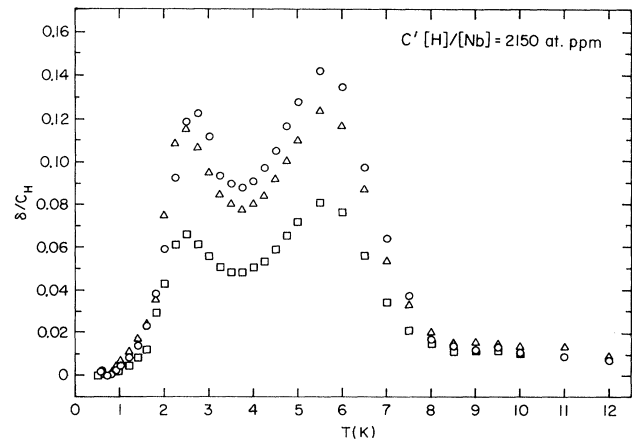


FIG. 7. Decrement of the C' mode per unit concentration as a function of temperature for $[H]/[Nb]=2150$ at. ppm after various quenches. Circles—1 K/min from room temperature. Squares—warmed to 150 K, followed by quench to 4 K. Triangles—warmed to 250 K, followed by quench to 4 K.

hydride to revert to solid solution. The sample was again cooled rapidly, about 10 K/min, and the decrement, represented by the triangles of Fig. 7, had regained most of its former magnitude. These results are interpreted as an indication that the concentration of oxygen-hydrogen pairs is variable, and depends upon the cooling rate. Since the concentration of hydrogen, which remains paired to oxygen and therefore contributes to the relaxation is not known, it is not possible to use Eq. (3) to derive the λ tensor elements which characterize the elastic interaction.

EFFECT OF OXYGEN CONCENTRATION

To determine the effect of the oxygen concentration upon the relaxation, the second sample Nb2, having a combined concentration of oxygen, carbon, and nitrogen of about 200 ppm, was charged with hydrogen to a con-

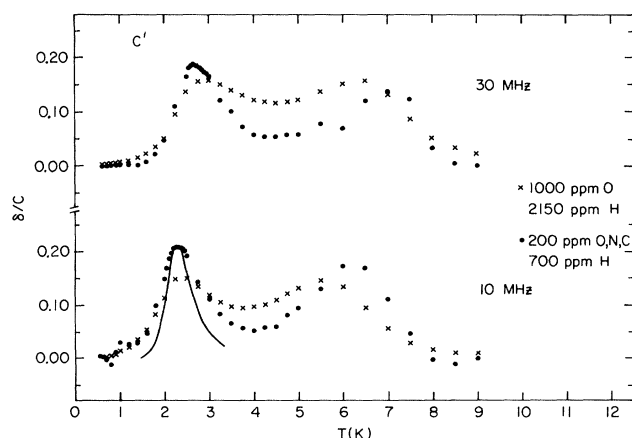


FIG. 8. Decrement of the C' mode per unit concentration as a function of temperature for two trap concentrations. Solid line under the low-temperature 10-MHz peak represents the expected shape of a relaxation with no broadening and with the observed activation energy.

centration of about 700 ppm. The objective of using smaller concentrations of these impurities was to reduce the internal strains produced by them, and to investigate the concentration dependence of the relaxation strength. The result can be seen in Fig. 8 for the C' mode at 10 and 30 MHz, compared to the previous results at higher oxygen concentration.

The most striking difference is the decrease in width and the higher values of the decrement per unit concentration for the relaxation peaks at a lower concentration of oxygen. This is consistent with a reduction in the width of the distribution of relaxation times. For comparison, the solid line in the lower curve near the 2.4-K peak indicates the expected result for a single relaxation with no broadening and with an activation energy equal to that observed for the low-temperature relaxation. The peak corresponding to the low trapping concentration conforms much more closely to the line than the peak for the higher trapping concentration. The temperature of the low-temperature peak is not significantly different for the two trap concentrations.

The high-temperature peaks do appear to be shifted to higher temperature with lower concentration of oxygen. Most of this shift is explained by the width of the peaks. In the high-oxygen-concentration curves, the low-temperature peak is broad enough to overlap the high-temperature peak. The falling tail of the low-temperature peak appears to shift the high-temperature peak to lower temperatures. Decreasing the oxygen concentration sharpens the peak, reducing the overlap, shifting the high-temperature peaks towards higher temperatures, and does not affect the temperature of the low-temperature peak. These results indicate that the strain fields due to adjacent oxygen solutes have the primary effect of broadening the spectrum of relaxation times but have no

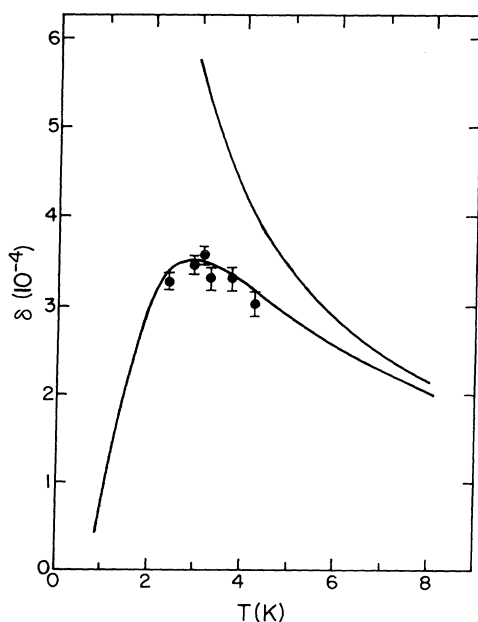


FIG. 9. Relaxation strength of the C' mode vs temperature for hydrogen.

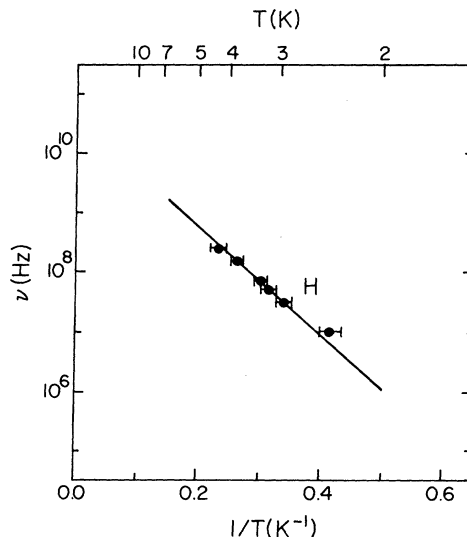


FIG. 10. Logarithm of relaxation frequency as a function of inverse temperature. Straight line is a fit to the data with an activation energy of 1.8 meV.

significant effect on the energy levels, which take part in the relaxations.

DISCUSSION

We confine ourselves here to the hydrogen-concentration-independent peak observed at 2.5 K at 10 MHz and will further discuss the higher-temperature peak in a subsequent publication. From the height and position of the peak, the temperature dependence of the relaxation strength and relaxation time can be obtained from Eqs. (2) and (3). These are shown in Figs. 9 and 10. The logarithm of the inverse of the hydrogen relaxation time

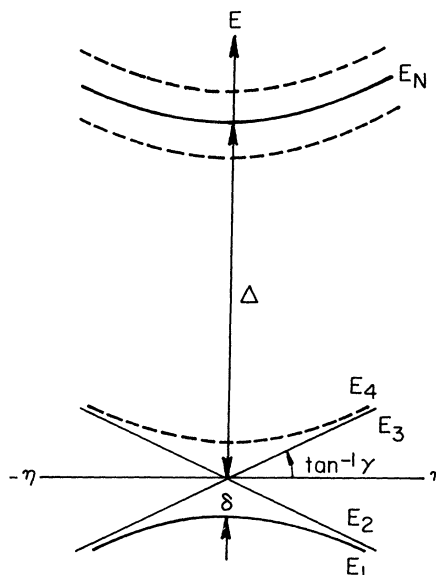


FIG. 11. Schematic diagram of an n -state tunnel system in which a degenerate first excited state is split by the strain η .

versus inverse temperature fits a straight line with an apparent activation energy of 1.8 meV (Fig. 10).

Figure 9 shows the relaxation strength as a function of temperature. Above 3 K the strength decreases with increasing temperature, which is consistent with the classical inverse temperature dependence in Eq. (3). However, below 3 K the strength also decreases, a departure from classical behavior. An interpretation of this effect in terms of a classical activation over a potential barrier cannot explain these observations. A model is needed which considers the properties of quantum-mechanical tunneling and can account for the interactions due to elastic strain.

The configuration of the O-H tunneling system is not known, nor is the number of equivalent sites making up the tunneling system known. These data, however, provide important clues and restrictions on the possible configuration. This can be illustrated by reference to Fig. 11, which is a schematic diagram of the strain dependence of an n -state tunneling system. The energy levels are given by

$$\begin{aligned} E_1(\eta) &= -[E_1(0)^2 + \gamma^2 \eta^2]^{1/2}, \\ E_{2,3}(\eta) &= \pm \gamma \eta, \\ E_i(\eta) &= [E_i(0)^2 + \gamma^2 \eta^2]^{1/2}, \quad i=4, n, \end{aligned} \quad (6)$$

where $E_i(0)$ is the energy of each level in the absence of strain and η is the strain.

The isothermal elastic change δC_{ij} is given by

$$C_{ij} = \frac{\partial^2 F}{\partial \eta_i \partial \eta_j}, \quad (7)$$

where $F = -nk_B T \ln Z$, n is the number of tunneling systems and Z is the partition function given by

$$Z = \sum_i \exp[-E_i(\eta)/k_B T]. \quad (8)$$

In general, the elastic-constant change consists of two parts, called relaxational and resonance parts, or paraelastic and diaelastic effects.²⁸ In the former case, an ultrasonic strain changes the energy levels so that the thermal-equilibrium distribution changes. If transitions can occur, the equilibrium is restored, and in the latter case an elastic-constant change occurs without transitions, for $\hbar\omega < E_2 - E_1$, because C_{ij} measures the curvature of the eigenstates, according to Eqs. (7) and (8).

For a two-state system consisting only of the levels E_1 and E_4 , only the diaelastic effect occurs for a small-amplitude ultrasonic strain about a zero-static-strain bias. This is because $\partial E_i / \partial \eta = 0$ for low strains and a small strain leads to no redistribution. At zero temperature only the ground state is occupied, so the elastic constant is given by the curvature of the ground state, which is negative. For higher temperatures, this negative contribution is decreased as the ground state is depleted at the expense of the higher state with positive curvature, and the effect disappears at high temperature. A redistribution, and therefore a relaxation, is possible for small ultrasonic strains about a static bias strain η_0 , but such a relaxation would have to be a direct transition with a relaxation rate which varied linearly with temperature, and could only

occur if the ultrasonic strain coupled with the two states to give a nonzero matrix element between them.²⁹

For a four-state system the levels $E_1 - E_4$, a relaxation could occur between the degenerate excited states E_2 and E_3 . If the transitions were direct, the rate would be linear in temperature. An indirect process is possible by absorption of a phonon to a higher state (E_4), followed by emission of a phonon to the state degenerate at $\eta=0$. This is known as an Orbach process³⁰ and occurs with a rate given by

$$\tau^{-1} = A \Delta^3 e^{-\Delta/k_B T}, \quad (9)$$

where Δ is the energy difference between the higher state and the degenerate relaxing state. Also the relaxation strength for the process would drop below the classical value at low temperatures when the excited state becomes depopulated. Most often, for a four-state system $|E_4(0)| = |E_1(0)|$ so that the characteristic energy δ for the disappearance of the relaxation strength would be the same as that Δ for the relaxation rate.

If the measured energy Δ is not $E_4 - E_3$, then an Orbach process might still proceed through a higher state E_n ($n > 4$). It has been shown⁹ that an elaboration of the Birnbaum-Flynn³¹ eight-state tunneling model to take account of the strain dependence leads to an energy-level structure which can be fit to the results found in the ultrasonic measurements. There are, however, still difficulties³² with the underlying configuration leading to this

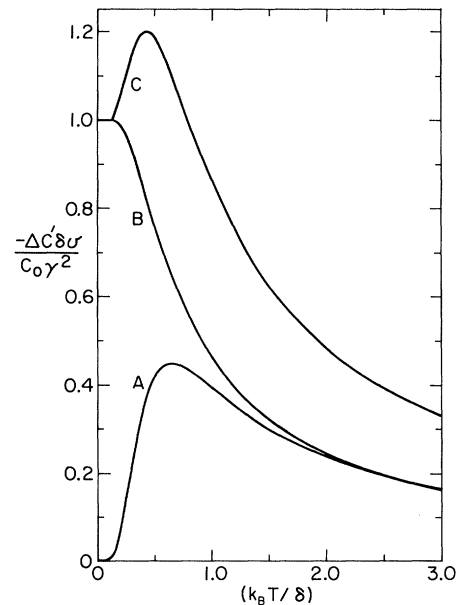


FIG. 12. Relaxation strength as a function of temperature for the system depicted in Fig. 10. Δ is the relaxation strength, δ is the energy difference between the ground and first excited states, v is the molecular volume, C_0 is the molar concentration of defects, and γ is the energy change of the first excited state with strain. Curve A represents the relaxation due to transitions between the degenerate first excited states (paraelastic). Curve B represents the contribution from the curvature of the ground state (diaelastic). Curve C is the sum of curves A and B.

energy-level structure, which will be discussed in a subsequent publication as well as another eight-state model which is consistent not only with the ultrasonic data, but with data from other sources. In the present we simply note that the relaxation strength at low temperatures will be mainly determined by the ground state and first excited states, given by Eq. (6), and characterized by the parameters δ and γ , while the relaxation time will be determined by Δ . The results of a calculation of the relaxation strength are seen in Fig. 12.

Curve *A* represents the contribution to the elastic constant due to the transitions between the degenerate states alone. At high temperatures it decreases as $1/T$, the same as a classical relaxation. As T approaches δ/k , the excited states begin to depopulate. This lowers the relaxation strength, which eventually goes to zero at $T=0$. This decrease of the relaxation strength due to depopulation is unique to quantum-mechanical systems and is not seen in classical relaxations.

Curve *B* is also unique. This contribution is derived from the second derivative of the ground-state energy with respect to C' strain. As seen in Fig. 11 the ground state has a negative second derivative with respect to strain. Since this contribution is not due to a relaxation between eigenstates, it is not a true relaxation. As long as the time required for the ground state to respond to applied stress is much shorter than one period of stress, the response will be in equilibrium and the calculation is valid. The total response is indicated by curve *C*, the sum of curves *A* and *B*. When the transition time between excited states is considered, the elastic-constant change is related by

$$-\delta C = \Delta_B + (\Delta_A / 1 + \omega^2 \tau^2), \quad (10)$$

where Δ_A and Δ_B are the functions represented by curves *A* and *B*. At high temperatures, where $\omega\tau$ is small, the elastic-constant change is given by curve *C*. At lower temperatures, where $\omega\tau$ increases, the elastic-constant change falls below curve *C* and approaches curve *B*, which it follows to the lowest temperature.

The ultrasonic measurements thus provide evidence that the configuration for Nb-O-H can be described as follows.

(i) There are sites equivalent by symmetry making up a quantum-tunneling system. This follows from the fact that the relaxation strength decreases below the classical $1/T$ dependence and a diaelastic effect appears in the elastic constant.

(ii) The relaxation appears in a degenerate excited state which lies 0.4 meV above the ground state. The degeneracy of this state is lifted by a C' -type, but not a C_{44} -type, strain.

(iii) The Arrhenius temperature dependence of the relaxation rate shows that an Orbach process occurs through an excited state at an energy $\Delta = 1.8$ meV. These results taken together show that the configuration consists of a minimum of, but probably more than four equivalent sites.

For Nb-O-D the relaxation is unusually broad and cannot be described by a single relaxation time. The relaxation rate appears to vary more slowly with temperature than for Nb-O-H.

SUMMARY AND CONCLUSIONS

The most important experimental results are the following.

(1) An anelastic relaxation due to hydrogen-oxygen complexes exists in niobium at temperatures near 4 K.

(2) The relaxation is absent in the C_{44} and bulk-modulus modes over an order of magnitude in hydrogen concentration.

(3) The relaxation is present in the C' mode at 2.4 K at 10 MHz for hydrogen with an apparent activation energy of about 1.8 meV.

(4) The deuterium relaxation is not of the Debye type, but shows a broad plateau with temperature. In addition, there exists a decrease in the elastic constant without a corresponding peak in the attenuation below 2 K.

(5) A second relaxation appears at higher hydrogen concentrations in the C' mode. The concentration dependence of the relaxation strength indicates a hydrogen pair defect, either isolated or possibly bound to an oxygen. The relaxation appears at 5.5 K at 10 MHz with an activation energy of 4 meV.

(6) The dependence of hydrogen concentration on cooling rate makes the concentration determination difficult. The relaxation strength remains the product of concentration and λ tensor. The relaxation strength is 2 or 3 orders of magnitude smaller than typical values for other defect systems.

(7) The relaxation strength of the hydrogen relaxation does not follow a normal $1/T$ dependence, but begins to decrease at the lowest temperatures.

The effects which are unusual for a relaxation, and which produce the most severe test for a model are the low temperature decrease in the elastic constant without a corresponding peak in the attenuation, the decrease of the hydrogen relaxation strength at low temperature, and the broadening of the deuterium peaks relative to the hydrogen peaks.

The measurements provide evidence that the configuration for Nb-O-H is a tunneling system consisting of a minimum of four equivalent sites. The symmetry is such that a C' -, but not a C_{44} -type, strain lifts the degeneracy of the first excited state.

ACKNOWLEDGMENTS

We thank A. C. Anderson for advice on the construction of the cryostat, H. J. Stapleton for discussion of the Orbach effect, and K. Huang for discussion of the interpretation of the results. This work was supported by the U.S. Department of Energy, Division of Materials Sciences, under Contract No. DE-AC02-76ER01198.

- ¹G. H. Sellers, A. C. Anderson, and H. K. Birnbaum, *Phys. Rev. B* **10**, 2771 (1974).
- ²C. Morkel, H. Wipf, and K. Neumaier, *Phys. Rev. Lett.* **40**, 947 (1978).
- ³C. Baker and H. K. Birnbaum, *Acta Metall.* **21**, 865 (1973).
- ⁴R. F. Mattas and H. K. Birnbaum, *Acta Metall.* **23**, 973 (1975).
- ⁵P. Schiller and A. Schneiders, *Phys. Status Solidi A* **29**, 375 (1975).
- ⁶P. Schiller and H. Nijman, *Phys. Status Solidi A* **31**, K77 (1975).
- ⁷C. G. Chen and H. K. Birnbaum, *Phys. Status Solidi A* **36**, 687 (1976).
- ⁸E. L. Andronikashvili, V. A. Melik-Shaknazarov, and I. A. Naskidashvili, *J. Low Temp. Phys.* **23**, 1 (1976).
- ⁹D. B. Poker, G. G. Setser, A. V. Granato, and H. K. Birnbaum, *Z. Phys. Chem. Neue Folge* **116**, 39 (1979).
- ¹⁰P. E. Zapp and H. K. Birnbaum, *Acta Metall.* **28**, 1275 (1980).
- ¹¹P. E. Zapp and H. K. Birnbaum, *Acta Metall.* **28**, 1523 (1980).
- ¹²G. Cannelli, R. Cantelli, and G. Vertechi, *Appl. Phys. Lett.* **39**, 832 (1981).
- ¹³G. Bauer, E. Seitz, H. Horner, and W. Schmatz, *Solid State Commun.* **17**, 161 (1975).
- ¹⁴N. Stump, G. Alefeld, and D. Tocchetti, *Solid State Commun.* **19**, 805 (1976).
- ¹⁵S. M. Shapiro, Y. Noda, T. O. Brun, J. Miller, H. Birnbaum, and T. Kajitani, *Phys. Rev. Lett.* **41**, 1051 (1978).
- ¹⁶D. Richter and S. M. Shapiro, *Phys. Rev. B* **22**, 599 (1980).
- ¹⁷H. Wipf, A. Magerl, S. M. Shapiro, S. K. Satija, and W. Thomlinson, *Phys. Rev. Lett.* **46**, 947 (1981).
- ¹⁸S. M. Shapiro, D. Richter, Y. Noda, and H. K. Birnbaum, *Phys. Rev. B* **23**, 1594 (1981).
- ¹⁹A. Magerl, J. J. Rush, J. M. Rowe, D. Riechter, and H. Wipf, *Phys. Rev. B* **27**, 927 (1983).
- ²⁰H. D. Carstanjen, *Phys. Status Solidi A* **59**, 11 (1980).
- ²¹W. F. Lankford, H. K. Birnbaum, A. T. Fiory, R. P. Minnich, K. G. Lynn, C. E. Stronach, L. H. Bieman, W. J. Kossler, and J. Lindemuth, *Hyperfine Interact.* **4**, 833 (1978).
- ²²S. G. O'Hara, G. J. Sellers, and A. C. Anderson, *Phys. Rev. B* **10**, 2777 (1974).
- ²³M. Locatelli, K. Neumaier, and H. Wipf, *J. Phys. (Paris) Colloq.* **39**, C6-955 (1978).
- ²⁴G. Pfeiffer and H. Wipf, *J. Phys. F* **6**, 167 (1976).
- ²⁵A. brief account of some of these results was given earlier in Ref. 9.
- ²⁶J. Holder, *Rev. Sci. Instrum.* **41**, 1355 (1970).
- ²⁷A. S. Nowick and W. R. Heller, *Adv. Phys.* **12**, 251 (1963); **14**, 101 (1965); A. S. Nowick and B. S. Berry, *Anelastic Relaxation in Crystalline Solids* (Academic, New York, 1972).
- ²⁸G. Matusiewicz and H. K. Birnbaum, *J. Phys. F* **7**, 2285 (1977).
- ²⁹A. V. Granato, in *Point Defects and Defect Interactions in Metals*, edited by J. Takamura, M. Doyama, and M. Kiritani (University of Tokyo Press, Tokyo, 1982), p. 67.
- ³⁰R. Orbach, *Proc. R. Soc. London Ser. A* **264**, 458 (1961).
- ³¹H. K. Birnbaum and C. P. Flynn, *Phys. Rev. Lett.* **37**, 25 (1976).
- ³²H. Wipf and K. Neumaier, in *Electronic Structure and Properties of Hydrogen in Metals*, edited by P. Jena and C. B. Satterthwaite (Plenum, New York, 1983), p. 485.